THERMAL EVOLUTION OF ENSTATITE CHONDRITE AND AUBRITE PARENT BODIES: CONSTRAINTS FROM SILICATE GEOTHERMOMETRY. E. N. Etheridge[1,2], B. A. Anzures[1,3], N. Dygert[4], C. A. Goodrich[1], F. M. McCubbin[3], M. Righter[5], R. Jakubek[6], M. Fries[3]. [1]Lunar and Planetary Institute/USRA (LPI), [2]Marietta College, [3]ARES, NASA Johnson Space Center [4]Dept. Earth & Planetary Sciences, University of Tennessee. [5]Dept. Earth & Atmospheric Sciences, University of Houston. [6]Jacobs JETS, NASA Johnson Space Center. Email: eetheridge31@outlook.com

Introduction: Enstatite chondrites (ECs) and aubrites experienced thermal metamorphism and possible fragmentation and reassembly of their parent bodies [e.g. 1,2]. ECs and aubrites (enstatite achondrites) are highly reduced, sulfur-rich meteorites primarily composed of orthopyroxene (opx), plagioclase (plg), clinopyroxene (cpx), silica polymorphs, sulfides, and kamacite (kam). ECs attained temperatures that produced petrologic types 3-7, while aubrites resemble igneous intrusive orthopyroxenite or norite cumulate rocks. It has been proposed that at least 8 parent bodies are necessary to explain the geochemical diversity in the current collection of ECs [3]. Texturally, ECs suggest their parent bodies experienced more severe thermal and shock metamorphism than other chondritic meteorites, however the thermal histories of ECs (especially peak temperatures and high temperature cooling rates) are poorly constrained. Current silicate equilibration temperature estimates range from 800-1000 °C for EH5 and EH6 chondrites. EL5 and EL6 chondrites may have experienced temperatures of 600-800 °C and aubrites may have experienced temperatures of ~1155 to ~1365 °C [1-4].

To understand the thermal evolution of enstatite chondrite and aubrite parent body/bodies, multiple thermometers are needed that are capable of distinguishing thermal histories through different temperature intervals, and potentially, between endmember models for parent body history and configuration: the onion shell and the rubble pile (the latter produced by fragmentation-reassembly events) [5,6]. Geothermometers and geospeedometers with differing temperature sensitivities [7-10] have been used to describe the thermal history of ordinary chondrites (OCs) [6] and four kinds of primitive achondrites [11,12], and we apply these same methodologies in this study to enstatite chondrites and aubrites.

Samples: We studied two ECs including EET 90102 (EL6) and Happy Canyon (EL6/7)] as well as two aubrites Larkman Nunatuk (LAR) 04316 and Lewis Cliff (LEW) 87020. The samples were acquired from NASA Johnson Space Center (JSC) and the American Museum of Natural History. Meteorite thick sections were mounted in epoxy and were polished in ethanol to 1 μm using diamond-embedded polishing paste.

Analyses: Cpx-opx and cpx-plg pairs were identified using a petrographic microscope and the PhenomXL Benchtop SEM at LPI. Elemental maps were produced with the JEOL 7600 SEM (15 kV and 20 nA) at NASA JSC. Elemental maps were converted to RGB and mineralogical maps in ImageJ and XMapTools as shown in **Fig 1**. Mineral major element compositions were acquired using the JEOL 8530 EPMA (15 kV and 25 nA) at NASA JSC. Opx, plg, and cpx trace element compositions were measured by LA-ICP-MS at the University of Houston (laser fluence of 3.95 J at 8-10 Hz with 10-20 ms count time and a spot size of 50-110 μm). Silica polymorphs were identified using a Witec Raman imaging microscope at NASA JSC.

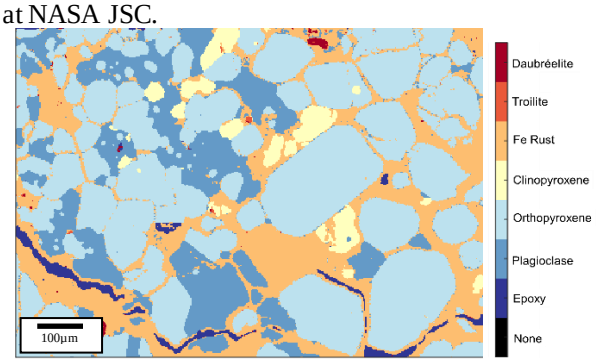

Figure 1. *Mineralogical map of cpx-opx and cpx-plg grain pairs in Happy Canyon, produced in XMapTools.*

Mineralogy: Cpx-opx and cpx-plg mineral pairs were identified in two type 6 ECs (EET 90102 and Happy Canyon) and two aubrites (LAR 04316 and LEW 87020), as cpx is rare in metamorphosed ECs. SiO_2 polymorphs including quartz, tridymite, cristobalite, and silica glass were identified as listed in **Table 1**.

Aubrites: Aubrites contain large subhedral to euhedral grains of opx (1mm-0.5cm), cpx (50μm-100μm), and plg (100μm-5mm) that display shock fracture textures. Kamacite (kam), sulfides, and other minor phases are present as anhedral grains (<10μm). LAR 04316 contains cpx-opx exsolution lamellae as well as silica glass. Interestingly, LAR 04316 is split into two major lithologies with one part largely composed of feldspathic glass as a newly identified aubrite basalt vitrophyre, which are rare basaltic residues of enstatite chondrite protoliths [13]. LEW 87020 also contains cpx grains with opx exsolution lamellae. The cpx grains are significantly larger in this sample than in LAR 040136. The interstitial silica polymorph in LEW 87020 is tridymite.

ECs: ECs have typically euhedral to anhedral grains of opx (10μm-300μm), cpx (10μm-50μm), and plg (10μm-100μm) occurring in both the matrix and highly brecciated recrystallized chondrules. ECs also contain

interstitial sulfides, metal, and silica polymorphs including cristobalite and quartz. Most of the cpx in this sample is within the recrystallized chondrules with crosscutting veins of Ca-sulfide and plg-rich material. EET 90102 has mostly smaller grains (<50μm) that are anhedral and homogenously distributed. EET 90102 also has tiny 1-2 μm melt inclusions in cpx indicative of incipient melting.

Table 1: *Calculated T_{Mg}* [9], *T_{BKN}* [7], *and T_{SiO2}* [2] *for meteorites with identified cpx grains.*

Sample	T_{BKN}	T_{Mg}	T_{SiO2}
Aubrites			
LAR04136	1010 ±63 °C	1012 ±3 °C	Glass (>1700 °C)
LEW87020	1090 ±30 °C		Tridymite (>867 °C)
Enstatite Chondrites			
EET90102 (EL6)	892 ±23 °C	1035 ±40 °C	Quartz (<867 °C)
Happy Canyon (EL6/7)	975 ±2 °C	1259 ±11 °C	Cristobalite (>1470 °C)

Temperatures and Cooling Rates: Silicate geothermometers used in this study take advantage of temperature sensitive partitioning of coupled elements to determine what temperature a mineral pair records. REE-based cpx-opx and cpx-plg thermometers often recover higher temperatures than major element thermometers because subsolidus diffusive exchange of REEs is many orders of magnitude slower than major elements.

Applying REE and major element thermometers can more completely clarify the thermal histories that ECs and aubrites experienced. Using the two-px thermometer developed by Brey & Köhler (T_{BKN}) [7] or the Mg-in-cpx-plg thermometer developed by Sun & Liang (T_{Mg}) [9], temperatures are similar to REE-based cpx-opx and cpx-plg thermometers as long as cooling rates were fast (i.e., quenching). The REE-based thermometers yield higher values if the system experienced slow cooling rates after peak metamorphic or igneous temperatures. If the major element temperatures are higher than the temperatures determined from the REE-based thermometers, the sample may record heating, or a chemical perturbation could have disturbed the mineral chemistry, creating inaccuracies in the calculated temperatures [8].

Two-pyroxene: Values calculated for the opx-cpx pairs examined in each sample using T_{BKN} are reported in **Table 1**. Aubrites show more intrasample variability between cpx-opx pairs using this thermometer due to the brecciated nature of this group, while the ECs are more consistent. Both groups have higher temperature than have been previously reported for aubrites and ECs.

Mg-in-cpx-plg: Values calculated for the cpx-plg pairs identified in the samples using T_{Mg} are reported in **Table 1**. The T_{Mg} temperatures only agree with T_{BKN} temperatures in LAR 04136. The other meteorites have $T_{Mg} > T_{BKN}$. This is consistent with plg forming after partial melting at a higher temperature (due to shock/impact melting), transient heating under subsolidus conditions, or chemical disturbance.

Silica polymorph thermometer: Kimura suggests that EL6/7's experienced high temperature metamorphism and partial melting to form cristobalite and tridymite [3]. Tridymite and cristobalite are stable above 867 ℃ and 1470 ℃ and were identified in LEW 87020 and Happy Canyon respectively, reflecting the high temperatures these samples must have experienced and subsequent fast cooling to preserve the high T silica polymorphs. Alternatively, the presence of quartz identified in EET 90102, which is stable below 867 °C, indicates an extended period of low temperature metamorphism if it is a product of the transition from tridymite or cristobalite. Silica glass in LAR 04316 indicates it experienced partial melting above the meteorite's solidus of ~1700 °C.

REE Temperature and Implications: Efforts to determine T_{REE} with new trace element data are ongoing. Data from Floss et al. [15] were used to calculate a REE-in-two-pyroxene temperature for EET 90102, recovering a T_{REE} around 1200 °C. For the measured grain sizes, the $T_{REE} >> T_{BKN}$ indicates a cooling rate of ~$3x10^{-3}$ °C/yr. This preliminary high temperature cooling rate is 2-4 orders of magnitude slower than the OC group (0.3-100 °C/yr) [6], but still faster than cooling rates relevant to onion shell parent bodies, which are 10^{-4} °C/yr or slower through the lower temperature intervals [5]. A cooling rate faster than an onion shell rate may reflect a collisional fragmentation event for the EET 90102 parent body at ≳900 °C. We find that the most thermally metamorphosed ECs and aubrites show complex thermal histories with some evidence of partial melting and significantly higher peak metamorphic or igneous temperatures than previously determined. This suggests that at least some EC and aubrite parent bodies underwent fragmentation events similar to OC parent bodies.

Acknowledgements: This work was supported by the LPI Summer Intern Program in Planetary Science and the LPI Cooperative Agreement.

References: [1] Zhang (1996) MPS, 31, 647-655. [2] Kimura (2010) MPS, 6, 855–868. [3] Weyrauch et al. (2018) MPS, 53, 394- 415. [4] Ray et al. (2021) Sci. Rep., 11, 22552. [5] Miyamoto (1981) Proc. LPSC, 1145- 1152. [6] Lucas et al. (2020) GCA 290, 366-390. [7] Brey & Köhler (1990) J. Pet. 31, 1353-1378. [8] Liang et al. (2012) GCA 102, 246-260. [9] Sun & Liang (2017) Contr. Min. Pet. 172, 1-20. [10] Sun & Lissenberg (2018) EPSL 487, 165-178. [11] Lucas et al. (2022) MAPS. [12] Anzures et al. (2022) LPSC LIII, Abstr. #2696. [13] Fogel (2005), GCA, 69, 1633-1648. [14] Cherniak & Liang (2007), GCA, 71, 1324-1340. [15] Floss et al. (2003), GCA, 67, 543-555.